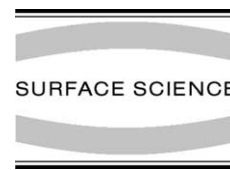




Available online at www.sciencedirect.com

SCIENCE @ DIRECT®

Surface Science 583 (2005) L142–L146



www.elsevier.com/locate/susc

Surface Science Letters

Structural characterization of nanopatterned surfaces

Michaël Lejeune ^{*}, Andrea Valsesia, Martin Kormunda, Pascal Colpo, François Rossi

Institute for Health and Consumer Protection (IHCP), Joint research Centre, European Commission, I-21020 Ispra (VA), Italy

Received 3 February 2005; accepted for publication 17 March 2005

Available online 7 April 2005

Abstract

In this work, chemically and topographically nanopatterned surfaces were produced by a top-down processing approach for biosensing devices. The nanopatterning was the result of the combination of plasma polymerisation (pp) of biofunctional materials and colloidal lithography techniques. The morphological and chemical properties induced by the plasma deposition–etching treatment were characterised by optical method combining ellipsometry and Fourier Transform Infrared spectroscopy studies. This method supported by atomic force microscopy measurements, allowed the full optical characterization of each step of the top-down process. The optical characterization of the end-up nanopatterned samples demonstrated that the chosen process is able to produce well-defined nanostructured surfaces with controlled chemical and morphological properties.

© 2005 Elsevier B.V. All rights reserved.

Keywords: Ellipsometry; Nanopatterning; Fourier transform infrared spectroscopy; Acrylic acid; Polymer; Atomic force microscopy

The reduction of the typical length scale in the creation of patterned surfaces is of high interest in the field of biointeracting materials and more particularly for biosensors designs. This has motivated several studies on the influence of the nanostructured materials on the protein adsorption or on the cell adhesion assays [1,2]. The technological difficulty relies in the creation of the nanostruc-

tures with controlled physico-chemical and geometrical properties, by exploiting the current nanofabrication techniques, which are potentially compatible with industrial scaling. The excellent results obtained by using a bottom-up approach (molecular assembly, auto-nanofabrication) are now far to be scaled to high-throughput systems [3]. On the other hand, top-down is giving very promising results but is often too expensive and time consuming (e.g. electron beam lithography [1]). In our approach we combined well-known techniques of material processing requiring fast

^{*} Corresponding author. Tel.: +39 0332 785497; fax: +39 0332 785487.

E-mail address: michael.lejeune@jrc.it (M. Lejeune).

fabrication steps, such as plasma based technique for etching and deposition of polymeric materials [4,5]. Nevertheless, the classical chemical characterizations such as X-ray photoelectron spectroscopy and time-of-flight secondary ion mass spectrometry (XPS/TOF-SIMS) have inherent physical limits for the lateral resolution, and so are inapt for the characterization of nanopatterned surfaces. For the characterization of such surfaces optical investigation techniques are often more sensitive and required small probe area. Ellipsometry are often used because it exhibits a high sensitivity and it is able to detect very small changes at the sub-nanometric level in the optical constants of the materials. In this article, we propose an optical method based on ellipsometry and Fourier transform infrared (FTIR) techniques enabling the characterization on chemically and topographically nanopatterned surfaces.

The engineering surface were produced using plasma based techniques (a schema of the process can be seen in Fig. 1). Plasma polymerised acrylic acid (ppAA) layers were deposited on intrinsic (100) silicon wafer assisted by pulsed plasma discharge of ultrapure acrylic acid (supplied by Aldrich, purity >99%), following the method previously described in Ref. [6]. Polystyrene (PS) beads (Aldrich, monodispersed in water, diameter = 500 nm \pm 50 nm) were then deposited on

the ppAA surfaces (Fig. 1a) as described in [7]. The sample was then exposed to oxygen plasma in a inductively coupled plasma (DICP) source until etching of around half diameter of the PS beads [7] (Fig. 1b). The ppAA and PS beads etching rates were accurately determined by a mechanical profilometer and scanning electron microscopy (SEM) measurements (LEO 435 VP). The etched surface was then covered with a 70 nm thick PEG-like layer in capacitively coupled plasma reactor (vapour precursor GLYME-2 supplied by Aldrich) (Fig. 1c). The sample was then washed in ultrapure water (Milli-Q, $r = 18 \text{ M}\Omega$) with ultrasounds for 4 min in order to detach the residual PS beads under the PEG-like coating (Fig. 1d). For each processing step, infrared spectrum and ellipsometric spectrum of the samples were acquired (always on the same analysis area) by using respectively a FTIR (Bruker Vector 22 in the wavelength range 400–4000 cm^{-1}) and a Variable Angle Spectrometric Ellipsometer (Nanofilm GmbH EP³ with a laser line at 532 nm with angle varying from 40° to 80° by steps of 0.5°). Before analysis, the baseline was substituted from each FTIR spectra using Airy functions. Ellipsometric spectra were fitted using the complex refractive index ($n + ik$) and the thickness as parameters. The surfaces were also analyzed for each step by atomic force microscope (NT-MDT with Si cantilever) for the morphological characterization.

Infrared spectra of samples after each processing steps are presented in Fig. 2. All infrared spectra show the typical characteristics of polyacrylic acid thin films [8,9]: two large bands around 1200 cm^{-1} and 1700 cm^{-1} respectively attributed to C–O and C=O and a very broad OH (2500–3300 cm^{-1}) band overlapping the CH_x stretching band (2800–3000 cm^{-1}). An intensive peak around 1650 cm^{-1} appears as a shoulder of C=O band and can be attributed to the CC double bond [9]. The presence of this last C=C peak can be due to the high crosslinking degree between the different polymeric chains of ppAA. After PS beads deposition on the ppAA film, Fig. 2a (black line curve), the shape of IR spectrum is not deeply modified. Nevertheless we observed the presence of several new peaks (indicated by * symbols in Fig. 2a): 695 cm^{-1} , 760 cm^{-1} , 2925 cm^{-1} and

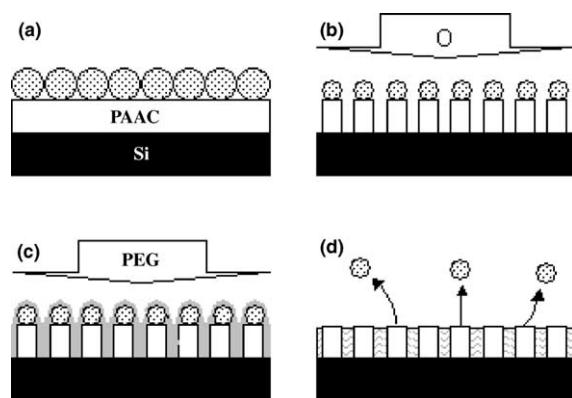


Fig. 1. Schema of the deposition process: (a) the PAAC layer deposited by plasma is covered by PS beads using spin coating, (b) oxygen plasma etching of the film, (c) PEG plasma deposition, (d) washing and removing of PS beads by ultrasonic bath.

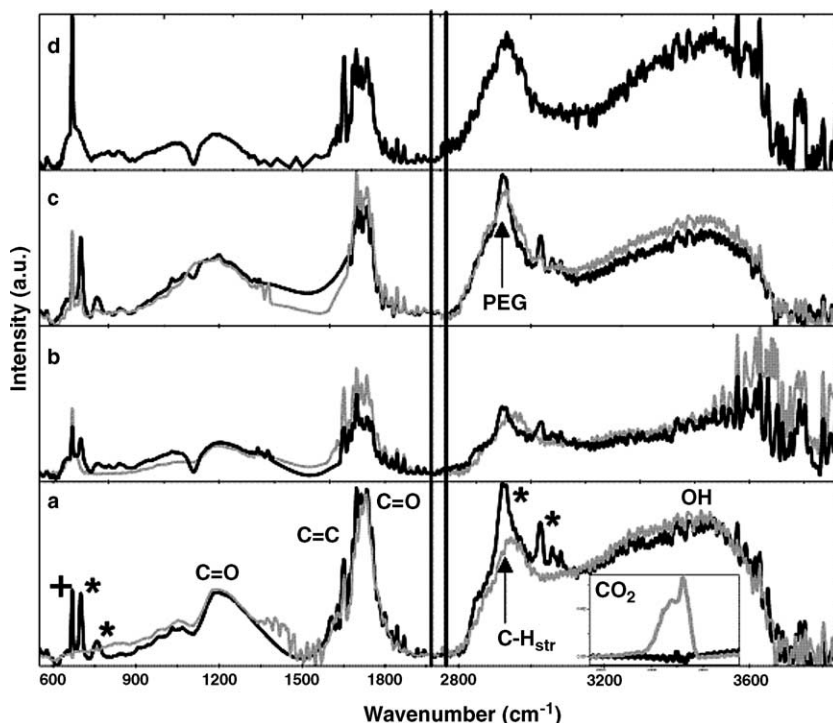


Fig. 2. FTIR spectra of sample after each processing step. In black ppAA + PS beads based samples and in gray samples deposited without PS beads: (a) as-deposited layers, in the box: CO₂ band between 2100–2500 cm⁻¹, (b) after etching process, (c) after PEG deposition, (d) final structure after cleaning phase. * symbols indicate the easily identifiable PS IR peaks, + correspond to the CO₂ peak.

3023 cm⁻¹, associated to the CH out of plane vibrations (doublet) and to CH stretching mode of PS [10]. The very narrow shape of these peaks is in good agreement with the initial good crystallinity of the manufactured PS beads. Although, the experimental conditions allow the quasi-suppression of atmospheric CO₂ on the infrared spectra, some peaks due to CO₂ atmospheric can be observed after deposition of PS beads (+ symbol and box in Fig. 2a): the doublet CO₂ 2330–2360 cm⁻¹ and a single peak around 665 cm⁻¹. Some CO₂ molecules are present into the structure of the sample, probably in the voids between the PS beads. After the next treatment step, the noise on the infrared spectra Fig. 2b increases. We can associate this phenomenon to the etching surface treatment that disorders the microstructure of the film. In one hand, the decrease of intensity of the different peaks and bands indicates that the thickness and/or the density of the film decrease,

but in an other hand confirms that after etching ppAA films and PS beads (PS are easily identifiable by the 695 and 3023 cm⁻¹ peaks) are always present. Due the closed IR absorption bands of PS and PEG, the PEG layer modifies weakly the infrared spectra of ppAA + PS samples, as seen in Fig. 2c (black curve). Nevertheless, by comparison between the spectra of samples ppAA (in gray in Fig. 2a) and ppAA + PEG (in gray in Fig. 2c) we can observe some change in the CH stretching band 2700–3100 cm⁻¹. After PEG deposition we observed a low shift and an enlargement of the main peak from 2930 to 2920 cm⁻¹, and an increase of the shoulder centred around 2885 cm⁻¹. These modifications can be attributed to PEG layer that shows vibration infrared bands at 2925 cm⁻¹ and 2884 cm⁻¹ [11]. After washing in ultrasonic bath, infrared spectra, Fig. 2d, the disappearance of the 695 cm⁻¹ and 3025 cm⁻¹ peaks confirms the complete removal of PS beads and

the CH stretching band always exhibits the contributions induced by ppAA and PEG. The final patterned structure is well built up by the two materials.

Infrared study gives some information about the material composing the sample but not on its architecture. We have chosen to complete the infrared characterization in using ellipsometry in complement. From ellipsometry measurements, thicknesses of ppAA layer and PS beads layer as described in Fig. 3a were determined around 350 nm and 520 nm respectively. ppAA thickness has been confirmed by profilometry and the value for the PS thickness is in good agreement with the diameter of beads. After the plasma etching, the surface is structured in three layers. The corresponding fitting of ellipsometry spectra, gives thickness of a ppAA layer of 150 nm, an intermediate layer of 200 nm and a surface layer of 160 nm. Using as a basis the previous AFM and SEM study of the nanodomains published by Valsecia et al. [7], we can relate the surface layer to a layer made up of etched PS beads. The intermediate layer with a low refractive index ($n = 1.1$) confirms a highly porous ppAA layer. One possible representation of this layer is a columnar pAAC

structure produced by the mask effect of the PS beads. Indeed, PS beads acting as masks, the initial ppAA layer has been only partially etched. The global thickness of the intermediate layer and the ppAA layer (200 nm and 150 nm) is closed to the initial PAAC layer (350 nm) and supports this hypothesis. Ellipsometry after PEG plasma deposition shows that PEG is deposited over the complete structure, event between the PS beads and the ppAA columna. The high coverage of the film by PEG is in good agreement with the strong PEG signal extracted from FTIR spectra. A schematic draw of the final structure is presented in Fig. 2c. We can see a four layers structure constituted by ppAA, ppAA + PEG, ppAA + PEG + air layers and a surface layer composed of PEG + air. The respective thicknesses of these layers were determined by ellipsometry spectra fitting. Calculated values are 150 nm, 127 nm, 80 nm and 21 nm for refractive index of 1.6, 1.51, 1.13 and 1. The designed structure exhibits a gradient of refractive index and indicates a decrease of the material density with the increase of the thickness. The presence of free spaces in the structure can be related to the presence of CO₂ observed on the FTIR spectra. Indeed, surfaces can trap CO₂

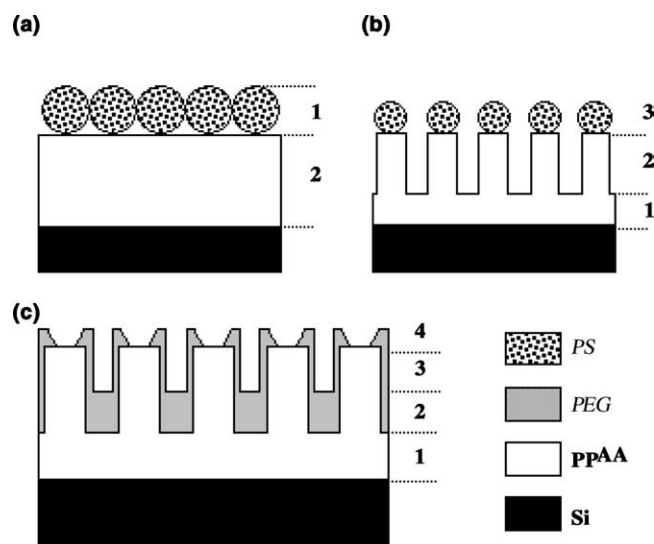


Fig. 3. Schematic view of the surface during the process top-down deduced from ellipsometry measurements. (a) as-dep ppAA + PS layer, (b) ppAA + PS layer after etching process: 1, ppAA layer; 2, ppAA columns; 3, etched PS, (c) columnar structure covered by PEG decomposed: 1, ppAA layer; 2, ppAA + PEG layer; 3, ppAA + PEG + air layer; 4, PEG + air layer.

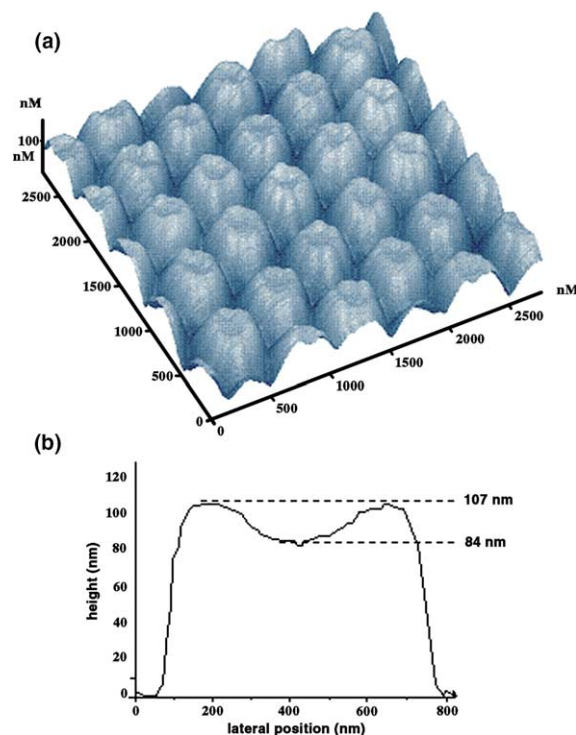


Fig. 4. (a) AFM micrography of the final structure. (b) Cross-section of a nanodome along the dashed line.

molecules from atmosphere inside the structure. The presence of a superficial layer with low thickness and a low refractive index indicates clearly that there is a structure with low density on the top of the domes. Ellipsometry does not allow having more information about this superficial structure. AFM micrography presented in Fig. 4 confirms the presence of a crater-like structure on the top of dome. The height of this crater around 20 nm and the height of the column of 84 nm correspond to the thicknesses calculated from ellipsometry measurements. The composition of the crater-like structure is for the moment unknown. But because of the total thickness of layers containing ppAA is really closed to the initial thickness of ppAA

deposited (around 350 nm), we can suppose that the border of the crater is formed by PEG during the third step of deposition.

In summary, a top-down processing approach, using combination of plasma and colloidal lithography techniques, permits the deposition of large nanopatterned surfaces. These large surfaces make easier the using of characterization techniques as FTIR or ellipsometry. The bi-material ppAA/PEG composition of the patterned film is clearly highlighted by the FTIR spectra. The final structure is more complex than suspected previously. But, the correlation between AFM and ellipsometry measurements allows having a good overview of the design and the forming of the nanostructure. The final layer is composed of ppAA nanodomes covered by PEG and crowned by a PEG nanocrater. As a consequence of these results it is plausible that the center of the nanocraters is constituted by as-deposited ppAA.

References

- [1] R.S. Kane, S. Takayama, E. Ostuni, D.E. Ingber, G.M. Whitesides, *Biomaterials* 20 (1999) 2363.
- [2] A.S. Blawas, W.M. Reichert, *Biomaterials* 19 (1998) 595.
- [3] H.G. Craighead, P.M. Mankiewich, *J. Appl. Phys.* 53 (1982) 7186.
- [4] N. Rossini, P. Colpo, G. Ceccone, K.D. Jandt, F. Rossi, *Mater. Sci. Eng. C* 23 (2003) 353.
- [5] C. Haginoya, M. Ishibashi, Kazuyuki Koike, *Appl. Phys. Lett.* 71 (20) (1997) 2934.
- [6] Dae-Geun Choi, Sarah Kim, Se-Gyu Jang, Seung-Man Yang, Jong-Ryul Jeong, Sung-Chul Shin, *Chem. Mater.* 16 (2004) 4208.
- [7] A. Valsesia, P. Colpo, M. Manso Silvan, T. Meziani, G. Ceccone, F. Rossi, *Nano Lett.* 4 (6) (2004) 1047.
- [8] V. Sciaratta, U. Vohrer, D. Hegemann, M. Muller, C. Oehr, *Surf. Coat. Technol.* 174–175 (2003) 805.
- [9] Hyun Il Kim, Sung Soo Kim, *J. Membr. Sci.* 190 (2001) 21.
- [10] A.A. Bhutto, D. Veselyb, B.J. Gabrysc, *Polymer* 44 (2003) 6627.
- [11] M. Manso Silvan, A. Valsesia, D. Gilliland, G. Ceccone, F. Rossi, *Appl. Surf. Sci.* 235 (2004) 119.